Research Paper

Journal of Engineering and Technological Sciences

Structure Simulation on Portable Commuter Bike Considering Frame Design and Materials Alternatives

Bambang Iskandriawan

Department of Industrial Design, Institut Teknologi Sepuluh Nopember, Sukolilo Keputih Campus, Surabaya 60111, Indonesia

Corresponding author: bisk@prodes.its.ac.id

Abstract

Portable commuter bikes (PCBs) are needed by commuters, people who live in the suburbs of a city and whose activities are in the middle of the city or vice versa, even for longer distances. For user safety, it is mandatory to check the strength aspect of the bicycle frame structure. PCBs are not only ridden by the commuter but can also be folded to bring them along on public transportation. The PCB design also included a stool to be used by the commuter while waiting for the bus or train. The strength of the PCB structure was investigated using numerical simulations based on static load. The displacements and stresses were controlled using a variety of PCB frame designs and materials. The results of this bicycle structural inspection can guide the improvement of PCB designs in the future.

Keywords: *bike structure; design alternatives; frame material; portable commuter bike; numerical simulation.*

Introduction

Commuters are city inhabitants who commute to a place for activities and return home every weekday. When the distance between the two locations is relatively long, apart from commuting using a bicycle, they may also use public transportation. The bike should be compact enough to fit into a bus or train. Safe and seamless operation of various modes of transportation in big cities, particularly in Indonesia, is a subject of study that must be conducted before the stakeholders make policy decisions [1] and [2]. The mapping results in [2] showed that the capital of a province in western Indonesia was better prepared for transportation system infrastructure arrangements compared to that of a province in eastern Indonesia. For portable commuter bikes (PCBs) to function optimally, it is necessary to plan for road infrastructure, mass rapid transportation (MRT), and reliable operators. The primary objective of this research was to develop a means of transportation the community requires, namely a PCB. MRT operations such as trains and buses can still be further optimized due to incomplete feeders in support of the MRT. In this case, the PCB serves as a feeder for the MRT and a means of short-distance transportation. PCBs can help commuters who live on the outskirts of a city get to their workplace in the city center or vice versa. Numerous bicycle design concepts have been realized and successfully commercialized [3,4]. The present research was strongly motivated by the advantages and disadvantages of various bicycle designs when designing and prototyping a PCB. The material selection strategy and design concept were carefully implemented to guide the research team [5,6].

There have been discussions on the design, structural, and operational aspects of several bicycle designs with a two-in-one concept, including the Trandem, Sliding Tandem Bike (STB), and Air Purifier Bike (APB) [7-9], while the present study focused on a PCB bike. These four different types of bicycles were designed and investigated to address societal problems. Client requirements play a crucial role in the valuation and judgment of intangible product design schemes. Consequently, firms should compile systematic information about customer constraints [10]. PCB bikes are developed to satisfy the needs of commuters who, in addition to folding their bikes to make them compact, want to sit on the bike when it is stationary. This study provides a structural strength analysis performed using numerical simulation methods. This information is important to consult when developing PCB designs. The requirement for using a folding bicycle is that the folding system design must be easy to operate, easy to move, and light enough for carrying the bicycle. The research team successfully

ISSN: 2337-5779

J. Eng. Technol. Sci. Vol. 55, No. 1, 2023, 12-21
DOI: 10.5614/j.eng.technol.sci.2023.55.1.2

DOI: 10.5614/j.eng.technol.sci.2023.55.1.2

fabricated an electric-PCB prototype, as shown in Figure 1. Apart from being foldable, the PCB includes a foldable seat that commuters can use while waiting for other modes of transportation or other purposes.

(a) (b) (c)

Figure 1 Electric portable commuter bike (e-PCB) prototype that was successfully realized by the research team in 2020, equipped with a seating facility (stool). Unfolded frame ready to ride (a), folded frame ready as a stool (b), and frame and steering folded for maximum compactness (c).

Each component dimension and the distance between the components on the bike were determined with the intended user in mind, not the other way around. Users who try to adjust it so that cycling becomes uncomfortable will increase the risk of accidents and even injury [11]. The task for the lower extremities can be altered by modifying the seat-tube angle. When the seat-tube angle is less than 90^o, a higher seat-tube angle can increase pedaling efficiency. A seat-tube angle greater than 90^o can promote recovery and exercise in the lower extremities [12]. Several ergonomic studies have been performed on folding bicycles. One important piece of information is that the optimal arrangement for male and female users is achieved with the steering wheel at 32 cm and the saddle at 83 cm in height [13]. One of the important things from the human factors aspect was the stool chair design specification for the PCB. In this paper, we report the analysis of displacement and stress that occurs due to static loading in the main frame of the e-PCB using numerical simulation methods.

Methods

The research method used was a numerical simulation. The finite element programming language used was ANSYS R18.2. The numerical simulation work for structure analysis of the PCB is shown step by step in Figure 2. It takes several repetitions to get the appropriate result for each stage. Analysis of the structural strength by numerical simulation methods is implemented for vehicles and buildings as places for human activities. An example of analyzing the model of an actual historical cathedral created by laser scans of its geometry was carried out by exploiting the finite element method [14]. The objective of the investigation was to assess the effects of fissuring destroying the brick buttress. Numerical simulation methods are reliable and capable of saving time and research costs.

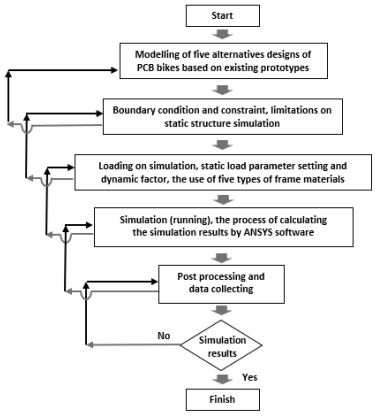

Figure 2 Workflow diagram of PCB bicycle structure analysis using numerical simulation method.

In a fairly complex model, there are thousands to millions of nodes and elements. Each node has a component of force, stress, strain, and displacement in the x, y, and z directions. The strain components in the three-dimensional model for each node are as follows (Eqs. (1) to (3)).

$$\varepsilon_{ij} = \frac{1}{2}\left(\frac{\partial u_i}{\partial x_j} + \frac{\partial u_j}{\partial x_i}\right) = \frac{1}{2}\left(u_{i,j} + u_{j,i}\right) \tag{1}$$

$$\varepsilon = \begin{bmatrix} \frac{\partial u_1}{\partial x_1} & \frac{1}{2}\left(\frac{\partial u_1}{\partial x_2} + \frac{\partial u_2}{\partial x_1}\right) & \frac{1}{2}\left(\frac{\partial u_1}{\partial x_3} + \frac{\partial u_3}{\partial x_1}\right) \\ \frac{1}{2}\left(\frac{\partial u_2}{\partial x_1} + \frac{\partial u_1}{\partial x_2}\right) & \frac{\partial u_2}{\partial x_2} & \frac{1}{2}\left(\frac{\partial u_2}{\partial x_3} + \frac{\partial u_3}{\partial x_2}\right) \\ \frac{1}{2}\left(\frac{\partial u_3}{\partial x_1} + \frac{\partial u_1}{\partial x_3}\right) & \frac{1}{2}\left(\frac{\partial u_3}{\partial x_2} + \frac{\partial u_2}{\partial x_3}\right) & \frac{\partial u_3}{\partial x_3} \end{bmatrix} \tag{2}$$

$$\varepsilon = \begin{bmatrix} \varepsilon_{xx} & \varepsilon_{xy} & \varepsilon_{xz} \\ \varepsilon_{yx} & \varepsilon_{yy} & \varepsilon_{yz} \\ \varepsilon_{zx} & \varepsilon_{zy} & \varepsilon_{zz} \end{bmatrix} \tag{3}$$

Each node or element of the model has the components of normal stress and shear stress as expressed in Eq. (4).

$$\sigma = \begin{bmatrix} \sigma_{xx} & \tau_{xy} & \tau_{xz} \\ \tau_{yx} & \sigma_{yy} & \tau_{yz} \\ \tau_{zx} & \tau_{zy} & \sigma_{zz} \end{bmatrix} \tag{4}$$

σ_{xx}, σ_{yy}, and σ_{zz} are the normal stresses and τ_{xy}, τ_{yx}, τ_{yz}, τ_{zy}, τ_{zx}, and τ_{xz} are the shear stress components respectively. In equilibrium conditions, the following equations will be obtained (Eqs. (5) to (8)).

$$\sigma_{ij,i} + \rho b_i = 0, \text{ or} \tag{5}$$

$$\frac{\partial \sigma_{xx}}{\partial x_1} + \frac{\partial \tau_{xy}}{\partial x_2} + \frac{\partial \tau_{xz}}{\partial x_3} + F_x = 0, \tag{6}$$

$$\frac{\partial \tau_{xy}}{\partial x_1} + \frac{\partial \sigma_{yy}}{\partial x_2} + \frac{\partial \tau_{yz}}{\partial x_3} + F_y = 0, \tag{7}$$

$$\frac{\partial \tau_{xz}}{\partial x_1} + \frac{\partial \tau_{xz}}{\partial x_2} + \frac{\partial \sigma_{zz}}{\partial x_3} + F_z = 0, \tag{8}$$

Furthermore, the von Mises stress is obtained as can be seen in Eq. (9),

$$\sigma_{Mises} = \sqrt{\frac{1}{2}\left[\left(\sigma_{xx} - \sigma_{yy}\right)^2 + (\sigma_{xx} - \sigma_{zz})^2 + \left(\sigma_{yy} - \sigma_{zz}\right)^2\right]} \tag{9}$$

The phenomena of displacement, strain, and stress can be observed using Hooke's law, where the force is the product of the spring constant and the displacement. In solid mechanics, the spring constant (k) is identical to the modulus of elasticity (E), and the displacement (Δl) is identical to the deformation. From the displacement value, the strain value can be obtained by using a reference before deformation occurs. Furthermore, the stress value can be obtained from the existing strain value (Eqs. (10) to (13)).

DOI: 10.5614/j.eng.technol.sci.2023.55.1.2

$$F = k.\Delta l \tag{10}$$

$$F = EA\ \frac{\Delta l}{l} \tag{11}$$

$$\varepsilon = \frac{\Delta l}{l} \tag{12}$$

$$\sigma = E\varepsilon \tag{13}$$

where *F* = force (N), *E* = elastic modulus (GPa), *⊿l* = length increase (m), and *l* = initial length (m) respectively.

Alternative PCB Frame Designs

Five new PCB frame designs were developed together based on an existing design (Figure 3). The PCB frame consists of five parts, for which alternative designs were considered: the head tube (A), the seat tube (b), the down tube (C), the seat stay (D), and the chainstay (E).

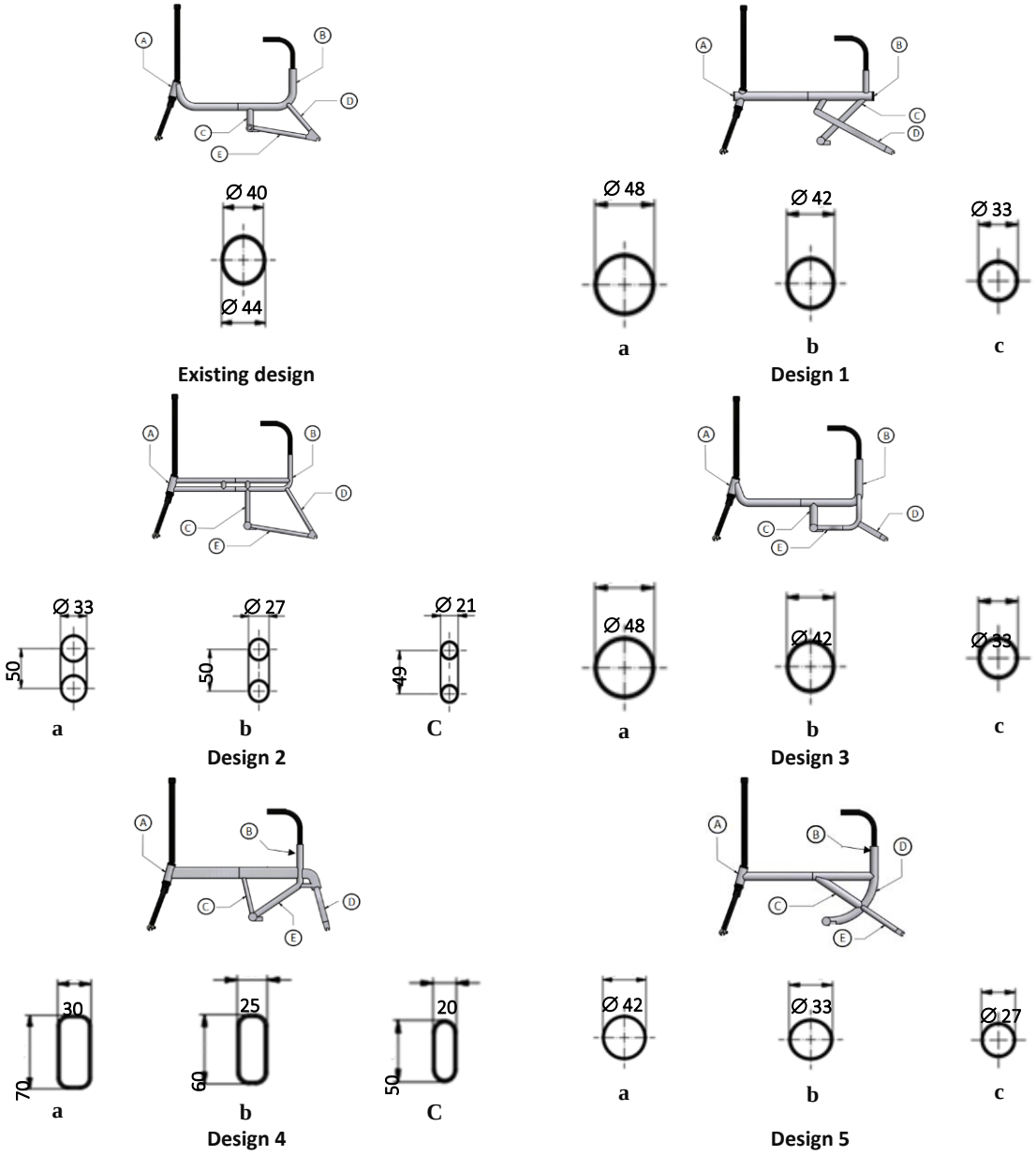

Figure 3 Existing PCB frame and five alternative designs along with their main cross-sectional dimensions (in mm).

The mainframe diameter of the existing design ∅ = 44 mm. The main frame of PCB frame design 1 is fundamentally different. Frame design 2 has a visible difference in the main frame. In their original design, mainframes A and B had two support pipes parallel to a single connecting pipe with three different diameters. Frame design 3 retains the design and shape of mainframes A and B, where the frame is curled downwards and joins the A and B frames. Additionally, design 3 includes three variants of the main frame diameter. The fourth frame design is significantly different from the existing design. Design 4 uses a hollow pipe with a quadrangular profile. The fifth frame is almost identical to design 1, only the mainframes A and B are straight in this design, with no downward curve.

Static Loading Model on the PCB

The bicycle legs connected to the wheel axle are 'fixed-support.' There are two fixed support points on the front and back, respectively. Static loading was applied to the seating area (saddle, point B) with a downward load of 1,500 N (y-), as shown in Figure 4. The frame load was obtained from the average weight of the Indonesian population multiplied by a factor of 2, i.e., around 1500 N.

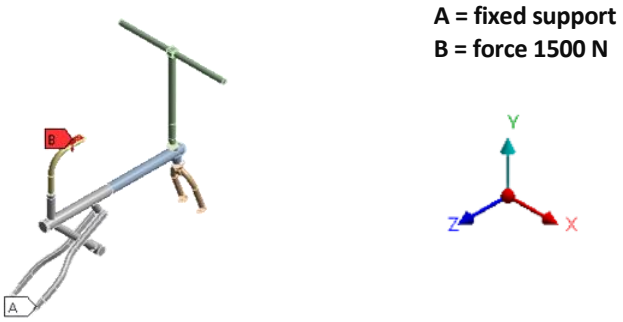

Figure 4 The location and magnitude of the load on the bicycle model at the time of the numerical simulation.

Material to be used in the Numerical Simulation Process

In addition to changing the shape and size of the bicycle frame design, the numerical simulation process included modifications to the type of bicycle frame material. Table 1 shows the selected material properties of the bicycle frame.

Table 1 Material properties were selected from five types of bicycle frame materials for the numerical simulation process [15].

Materials	Elastic Modulus, E (GPa)	Yield Tensile Strength, σ_Y (MPa)	Ultimate Tensile Strength, σ_U (MPa)	Poisson's Ratio
Structural steel	200	250	460	0.3
Aluminum alloy	68.9	266	290	0.35
Titanium alloy	103	275	345	0.34
Carbon fiber	221	3100	3500	0.2
Tectona grandis	10.7	110	118	0.11

Results and Discussion

Maximum Displacement on PCB Frame

Strain is the response of a material to a given force or stress. The strain value is determined by the modulus of elasticity and the amount of stress exerted on the material geometry. The greater the value of the modulus of elasticity, the quantity of the strain that occurs will be smaller. The amount of strain can be seen from the deformation value in the geometry or frame. Inspection of material displacement in the equipment is required to control the static load when in use.

Figure 5 shows the results of measuring the maximum displacement (δ_{max}) on the PCB frame by numerical simulation using aluminum alloy with a medium dimension (design b). All the biggest maximum displacement

DOI: 10.5614/j.eng.technol.sci.2023.55.1.2

PCB occurred at the top of the seat tube, which is the area closest to the static load. The biggest maximum displacement occurred in design 3b, i.e., 11.6 % greater than that in the existing design. The smallest maximum displacement occurred in design 4b, i.e., 37.9 % smaller than that in the existing design. Therefore, the best design from the point of view of maximum displacement was 4b, where the action of bending deformation on the welds was quite significant [16].

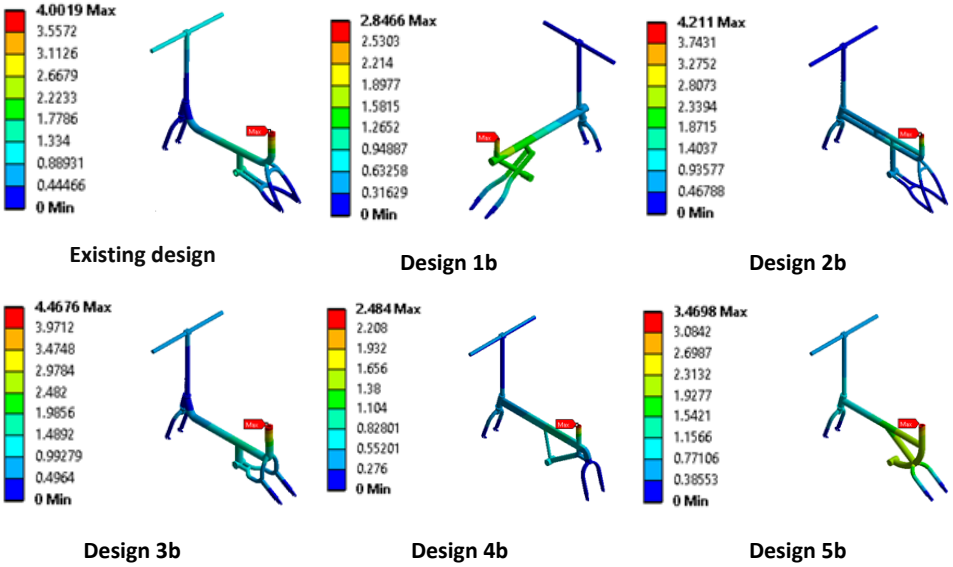

Figure 5 The locality of the maximum displacement (red signs) that occurs during loading in the six-frame designs when using aluminum alloy.

Table 2 shows a comparison of each design with the frame dimensions from the aspect of the maximum displacement obtained by the numerical simulation. Normally, reducing the dimensions of the cross-section of the frame will increase the maximum displacement that occurs. The bold gray boxes show when the maximum displacement was higher than that of the existing design frame, while the gray boxes show when the maximum displacement was lower than the existing one. Design 4 was the best in this regard.

Table 2 Maximum displacement in the PCB for several styles of frame designs by using five different materials. The designer needs to be careful because some of the new designs turned out to have a very high displacement.

Materials		**Structural steel**	**Aluminum alloy**	**Titanium alloy**	**Carbon fiber**	**Tectona grandis**
Elastic Modulus, E (GPa)		200	68.9	103	221	10.7
Alternatives design		Maximum displacement, δ_{max} (mm)				
Existing design		1.43	4.00	2.94	0.28	23.24
1	a	0.91	2.55	1.88	0.18	14.75
	b	1.01	2.85	2.10	0.20	16.48
	c	1.58	4.44	3.28	0.31	25.73
2	a	0.96	2.71	2.01	0.19	15.66
	b	1.51	4.21	3.11	0.29	24.37
	c	2.46	6.92	5.11	0.48	40.10
3	a	1.02	3.38	2.49	0.24	19.58
	b	1.59	4.47	3.29	0.32	25.88
	c	3.02	8.71	6.42	0.61	50.43
4	a	0.52	1.47	1.09	0.10	8.52
	b	0.88	2.48	1.83	0.18	14.37
	c	1.11	3.10	2.29	0.22	17.93
5	a	0.75	2.10	1.56	0.15	12.15
	b	1.23	3.47	2.56	0.25	20.06
	c	1.75	4.94	3.64	0.35	28.56
Average		1.36	3.86	2.85	0.27	22.36

The maximum displacement value was still below that of the original frame design, even when reducing the frame dimensions. The use of a pipe frame with a rectangular cross-section can be considered if the designer wants to reduce the deformation in the bicycle frame. Reduction of the dimensions of the mainframe in designs 1, 2, 3, and 5 is very prone to increase the deformation. Tectona grandis is not recommended as a material for the bicycle frame, because the displacements that occurred were very large, i.e., $\delta_{max\ average}$ = 22.36 mm, more than 16 times the maximum displacement that occurred when using structural steel. Structural steel, aluminum alloy, and titanium alloy materials had an average maximum displacement of $\delta_{max\ average}$ = 2.69 mm. The carbon fiber material was the best, with a $\delta_{max\ average}$ of only 0.27 mm.

Maximum Stress and Safety Factor of PCB Frame

The simulation results were used to determine the stress value for each design. In this case, what is meant by stress is von Mises stress. Material stress in the product must be measured to determine the static loading when the product is in use. Figure 6 shows the numerical simulation results used to control the maximum stress (σ_{max}) in the bicycle frame. In almost all PCB designs, the highest stress occurred in the seat-tube area, except for designs 3 and 5, where the maximum stress occurred in the frame end area.

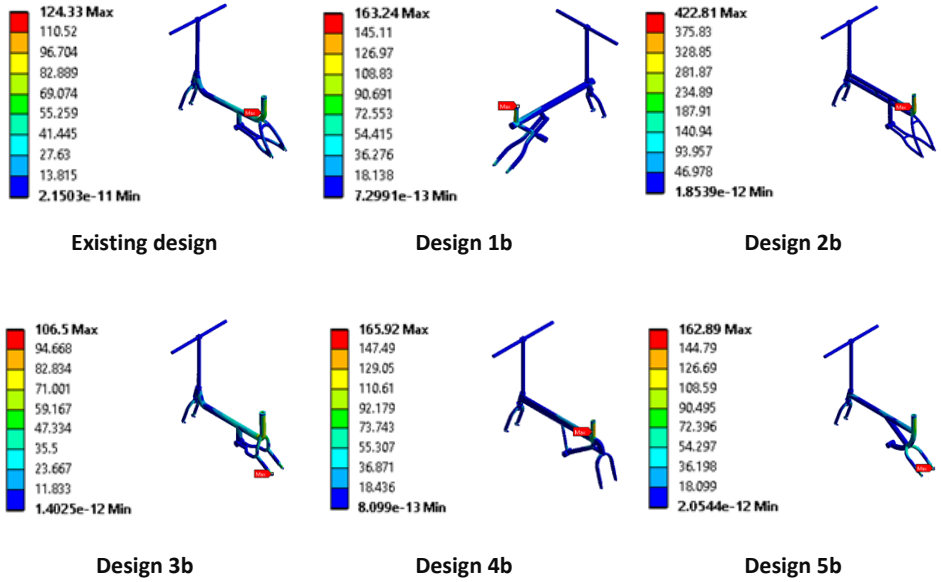

Figure 6 The location of maximum stress (red signs) that occurred during PCB loading for the six-frame designs using aluminum alloy.

The maximum stress in the frame end area was quite high due to the angle of the frame end to the horizontal plane being sharp and not supported by other parts of the frame (chainstay). This does not create a closed structure. Although the frame end of design 4 is almost identical to that of designs 3 and 5, it forms a large angle with the horizontal plane. The largest maximum stress (σ_{max}) occurred in design 2b, i.e., 240.1% greater than in the existing design. The lowest maximum stress (σ_{max}) occurred in design 3b, i.e., 14.3% smaller than in the existing design. The best design from the point of view of maximum stress was 3b. The material behavior used in the numerical simulation was elastic linear. This condition was used because almost all the stresses that occurred were still below the yield limit of each material.

The alternative design, along with each frame's dimensions from the aspect of the maximum stress for aluminum alloy followed by the safety factor for each bicycle frame material from the numerical simulation can be seen in Table 3. The orange boxes indicate when the maximum stress (σ_{max}) exceeded that of the existing design. The red box indicates when σ_{max} surpassed the yield tensile strength (σ_Y), except for the carbon fiber material. Several safety factors indicate that the value was equal to or smaller than 1, a very unexpected condition.

The lowest maximum stress occurred in frame design 3, which may also mean that design 3 is the most durable. Unfortunately, reducing the dimensions of the pipe cross-section will also result in the maximum stress

DOI: 10.5614/j.eng.technol.sci.2023.55.1.2

exceeding that of the existing design. The rounding at certain corners in frame design 3 is enough to make the frame sufficiently sturdy. Frame designs 1 and 2 are the weakest. In contrast, the sharp corners in frame design 1 and the double pipe with a relatively small diameter in frame design 2 weaken the structure. An interesting phenomenon occurred in design frame 1. The reduction in the dimensions of the frame strengthened the structure. This is caused by the concentration of stress in the meeting areas with other pipe parts. Reducing the cross-section of the pipe will strengthen these, but there is an optimal point. If the dimensional reduction continues, the maximum stress will increase again, a given that requires special attention from bicycle frame designers. Rather extreme conditions also occurred in frame design 5. A decrease in certain dimensions of the pipe cross-section resulted in a relatively large strength (design 5c).

Table 3 The safety factors that occurred for the various PCB frame designs using five different materials, where some of the new designs require special attention when reducing the dimensions because several designs with certain materials do not take the safety factor into account (printed in red).

Materials		**Aluminum alloy**	**Structural steel**	**Aluminum alloy**	**Titanium alloy**	**Carbon fiber**	**Tectona grandis**
Yield Tensile Strength, σ_y (MPa)		266	250	266	275	3100	110
Alternatives design		Maximum Stress (MPa)	Safety Factor (SF)				
Existing design		124.33	2.0	2.1	2.2	24.9	0.9
1	a	183.41	1.4	1.5	1.5	16.9	0.6
	b	163.24	1.5	1.6	1.7	19.0	0.7
	c	482.24	0.5	0.6	0.6	6.4	0.2
2	a	167.16	1.5	1.6	1.6	18.5	0.7
	b	422.81	0.6	0.6	0.7	7.3	0.3
	c	470.16	0.5	0.6	0.6	6.6	0.2
3	a	96.77	2.6	2.7	2.8	32.0	1.1
	b	106.50	2.3	2.5	2.6	29.1	1.0
	c	153.65	1.6	1.7	1.8	20.2	0.7
4	a	110.43	2.3	2.4	2.5	28.1	1.0
	b	165.92	1.5	1.6	1.7	18.7	0.7
	c	187.67	1.3	1.4	1.5	16.5	0.6
5	a	144.65	1.7	1.8	1.9	21.4	0.8
	b	162.89	1.5	1.6	1.7	19.0	0.7
	c	774.99	0.3	0.3	0.4	4.0	0.1
Average			1.5	1.5	1.6	18.0	0.6

Further, to examine the acclimatization of interaction stress within the rope strand, the ANSYS software was used to review the locations of contact pressure and resistance stress. These were obtained from the distribution maps of the contact pressure and friction stress in the string under workable capacity [17]. Observing the five new designs based on the kind of material, especially from a safety factor point of view, again the carbon fiber was the best-performing material, while tectona grandis performed the worst, where the safety factor was only 0.6. On the other hand, the safety factor for carbon fiber was more than 12 times that for structural steel. Wood as a replacement material has been quite successful, for example for snap-fit components [18], but it does not apply to bike designs.

The maximum displacement (δ_{max}), maximum stress (σ_{max}), and safety factor (SF) in each design can be seen in Tables 2 and 3 for the five selected materials. The maximum displacement difference that occurred in these materials between the largest and the smallest value was very large, i.e., more than 80 times. Tectona grandis elongated the most, i.e., 23.22 mm, while carbon fiber was shortened the most, i.e., 0.28 mm. The lower the modulus of elasticity (E) tended to be, the larger the deformation that occurred. In this case, tectona grandis is not safe for use in this bicycle design. Special treatments, such as injections, must be performed on the material to make it more difficult to stretch. The maximum stress quantity was relatively the same. The difference in the yield tensile strength (σ_y) of structural steel, aluminum alloy, titanium alloy, carbon fiber, and tectona grandis materials, i.e., 250, 266, 275, 3100, and 110 MPa, respectively, resulted in a significant difference in safety factor. The tectona grandis material had the lowest safety factor (SF = 0.6), while the carbon fiber material had the best

safety factor (SF = 18.0). There has been no discussion concerning the safety factor in previous works, especially related to bicycles with a two-in-one concept. They only discussed maximum displacement and stress for various bicycle designs and materials.

Conclusion

The conclusions that follow the PCB structure analysis are an invaluable provision for further PCB design development. Improving the PCB design will attract more customers and better prepare for products downstream while maintaining control over the bicycle structure's strength.

In general, decreasing the dimensions of the PCB frame ∅ will be followed by an increase in the maximum displacement (δmax) that occurs. Special designs, such as using pipes with a rectangular cross-section, can achieve a good maximum displacement while also reducing the pipe dimensions. Frames with a rectangular cross-section will be more robust than frames with round or oval pipes. The maximum displacement that occurred in carbon fiber was very low, i.e., only 0.27 mm, and it was the highest in tectona grandis, i.e., equal to 22.36 mm. Structural steel, aluminum alloy, and titanium alloy had almost the same maximum displacement, with an average rate of 2.69 mm (12.03%) of the maximum displacement occurring in tectona grandis). The occurrence of maximum displacement in the PCB for each material is strongly influenced by its elastic modulus. The lower the elastic modulus, the greater the maximum displacement in the PCB frame.

It is acceptable to increase the variety of PCB designs in reducing the size of the pipe cross-section, as this results in a slimmer design and lighter weight. However, there is an optimal point, where further reducing the dimensions of the PCB frame pipe ∅ increases the maximum stress, which occurs most frequently when it exceeds the yield tensile strength. Such conditions must be avoided. Particularly for high-risk designs, such as sharp corners in the bicycle frame, a slight decrease in frame dimensions can significantly increase the maximum stress. The difference in the material used, in this case of the yield tensile strength (σy), can be used to control the value of the safety factor. Carbon fiber is the most reliable choice in terms of safety factors. The value is quite safe, i.e., equal to 18.0, or almost 4 times the average safety factor of structural steel, aluminum alloy, and titanium alloy, and even 30 times that of tectona grandis. Tectona grandis is not recommended as a bike frame material in terms of the safety factor and maximum displacement.

Acknowledgments

Funding for this work was provided by the Ministry of Education, Culture, Research, and Technology, the Republic of Indonesia, through the National Competitive Applied Research (PTKN) scheme.

References

[1] Lawalata, G.M. & Agah, R.A., *Traffic Conflict Analysis as a Road Safety Diagnostic Tool for Urban Road Facilities*, International Journal of Technology, **2**, pp. 112-121, 2011.

[2] Latief, Y., Berawi, M.A., Rarasati A.D., Supriadi, L.S., Berawi, A.R.B. & Hayuningtiyas, I.S., *Mapping Priorities for the Development of the Transportation Infrastructure in the Provincial Capitals of Indonesia*, International Journal of Technology, 4, pp. 544-552, 2016.

[3] Wiyancoko, D., *Indonesian Bicycle Design*, KPG (Gramedia Popular Library) Jakarta, ISBN: 978-979-91-0243-0, 2010. (Text in Indonesian)

[4] Embacher, M., foreword by Paul Smith, *Cyclepedia, A Tour of Iconic Bicycle Designs*, Thames & Hudson, ISBN 978-0-500-51558-7, 2011.

[5] Cross, N., *Engineering Design Methods, Strategies for Product Design, Second Edition*, John Wiley & Sons Ltd, Baffins Lane, Chichester, West Sussex, PO19, England, 1998.

[6] Ashby, M. & Johnson, K., *Materials and Design, The Art and Science of Material Selection in Product Design*, Butterworth Heinemann, Oxford, UK, 2007.

[7] Iskandriawan, B. & Jatmiko, *The Development of Bicycles into Trandem: The Bike Can Be Used as A Tandem or Single Depending on the Necessity*, Applied Mechanics and Materials, **607**, pp. 920-925, 2014.

DOI: 10.5614/j.eng.technol.sci.2023.55.1.2

[8] Iskandriawan, B., Jatmiko, Windharto, A. & Krisbianto, A.D., *Mainframe Structure Exploration of Sliding Tandem Bike as The Effort to Enhance Product Features*, Journal of Engineering and Applied Sciences, **13**(7), pp. 1872-1876, 2018.

[9] Iskandriawan, B., Jatmiko, Safaat, A. & Nugroho, J.A., Air Velocity and Pressure Drop Exploration Inside Pipe Frame of Air Purifier Bicycle using Numerical Analysis, Journal of Engineering Science and Technology, 15(6), pp. 3935-3954, 2020.

[10] Huang, H.Z., Li, Y., Liu, W., Liu, Y. & Wang, Z., *Evaluation and Decision of Products Conceptual Design Schemes Based on Customer Requirements*, Journal of Mechanical Science and Technology, **25**(9), pp. 2413-2425, 2011.

[11] Laios, L. & Giannatsis, J., *Ergonomic Evaluation and Redesign of Children Bicycles Based on Anthropometric Data*, Applied Ergonomics, **41**(3), pp. 428-435, 2010.

[12] Chen, C.H., Huang, Y.H. & Shiang, T.Y., *The Effect of Bicycle Seat-Tube Angle on Muscle Activation of Lower Extremity*, Journal Science and Cycling, **4**(1), pp. 28-32, 2015.

[13] Muslim, E., Nurtjahyo, B. & Ardi, R., *Ergonomic Evaluation of a Folding Bike Design Using Virtual Environment Modelling*, International Journal of Technology, **2**, pp. 122-129, 2011.

[14] Cicero, S., Lacalle, R., Cicero, R., Fernández, D. & Méndez, D., *Analysis of the Cracking Causes in an Aluminum Alloy Bike Frame*, Engineering Failure Analysis, **18**(1), pp. 36-46, 2011.

[15] Anderson, T.L., *Fracture Mechanics Fundamentals and Applications*, Third Edition, Taylor and Francis Group, LLC, U.S., 2005.

[16] Wu, C., Lee, C. & Kim, J.W., *Numerical Simulation of Bending Deformation Induced by Multi-Seam Welding of a Steel-Pipe Structure*, Journal of Mechanical Science and Technology, **34**(5), pp. 2121-2131, 2020.

[17] Wang, H., Fu, C., Cui, W., Zhao, X. & Qie, S., *Numerical Simulation and Experimental Study on Stress Deformation of Braided Wire Rope*, The Journal of Strain Analysis for Engineering Design, **52**(2), pp. 69-76, 2017.

[18] Samboro, M.Y.A. & Kuswanto, D., *Snap-Fit Joinery System Using Pinewood Material Elasticity Properties*, Journal of Engineering and Technological Sciences, **52**(6), pp. 798-804, 2020.

Manuscript Received: 7 June 2022
1st Revised Manuscript Received: 10 October 2022
2nd Revised Manuscript Received: 1 December 2022
Accepted Manuscript: 26 January 2023